Microwave dielectric properties and low temperature sintering of $Ba_3Ti_{4-x}(Mg_{1/3}Nb_{2/3})_xNb_4O_{21}$ ceramics with $BaCu(B_2O_5)$ addition

Jinjin Zhang · Ruzhong Zuo · Yang Lv · Yuanyuan Zhou · Zhenxing Yue

Abstract Microwave dielectric ceramics of Ba_3Ti_{4-x} $(Mg_{1/3}Nb_{2/3})_xNb_4O_{21}$ solid solutions (BTMNN-x, x = 0–4) were prepared via the conventional solid-state reaction method. The X-ray powder diffraction analysis revealed that the BTMNN-x ceramics formed complete solid solutions with hexagonal structure. The dielectric constant (ε_r) and the temperature coefficient of the resonant frequency (τ_f) of BTMNN-x ceramics decreased with the increase of x, while the quality factor (Q × f) enhanced with increasing the substitution content. In addition, a small amount of $BaCu(B_2O_5)$ (BCB) additive can effectively lower the sintering temperature of BTMNN ceramics. The 1.5 wt% BCB doped BTMNN-2 ceramics can be sintered at 950 °C and have good microwave dielectric properties of $\varepsilon_r = 50$, Q × f = 10,500 GHz and $\tau_f = 18$ ppm/°C, which makes it possible to be a promising candidate for mid-permittivity low temperature co-fired ceramic materials.

1 Introduction

With the rapid growth of advanced communication systems, low temperature co-fired ceramics (LTCC) technology that are used for novel multi-layer communication modules has become the excellent solution for mobile and satellite communication systems. The critical requirements for LTCC materials are low sintering temperature (below 960 °C), good microwave dielectric properties, as well as excellent chemical compatibility with electrode materials [1]. Several microwave dielectric ceramic systems, including $ZnNb_2O_6$, $MgO-TiO_2$, $BaO-TiO_2$, $Ca[(Li_{1/3}Nb_{2/3}),Ti]O_{3-\delta}$, $Li_2O-Nb_2O_5-TiO_2$ and $BaO-Ln_2O_3-TiO_2$ (Ln = La, Nd, Sm) system have been reported for applications using low-melting glass frits or oxides [2–7]. However, among the reported LTCC systems, the mid-permittivity LTCC materials with high dielectric constant ($\varepsilon_r \geq 45$) and high Q × f (Q × f≥10, 000 GHz) value are few because high ε_r values usually cause high dielectric loss.

Sebastian [8] first reported the microwave dielectric properties ($\varepsilon_r = 55$, Q × f = 9,000 GHz, $\tau_f = 100$ ppm/ °C) of the $Ba_3Ti_4Nb_4O_{21}$ (BTN) ceramic in $BaO-TiO_2$-Nb_2O_5 system. BTN has the hexagonal crystal structure and belongs to the family of $A_3M_8O_{21}$ (A = K, Ba; M = Nb, Ti, Cr, Fe, Ni, Mg, Zn) [9]. This material is adequate for practical usage because of its large temperature coefficient of the resonant frequency (τ_f). Several studies were carried out to tune its microwave dielectric properties. However, either the τ_f value was still quite positive (~ 50 ppm/°C) or the Q × f values decreased seriously [10–12]. Recently, Zhang et al. [1] reported that they had efficiently modified the microwave dielectric properties of BTN ceramics by substituting $(Zn_{1/3}Nb_{2/3})^{4+}$ for Ti^{4+} ($\varepsilon_r = 65-45$, Q × f=12,000–16,000 GHz, $\tau_f = 90-10$ ppm/°C). It is known that ZnO evaporates easily at high temperature. Mg element has the similar chemical properties with Zn element but MgO does not evaporate during sintering. To obtain better microwave dielectric properties, we have prepared $Ba_3Ti_{4-x}(Mg_{1/3}Nb_{2/3})_x$ Nb_4O_{21} (BTMNN-x, x = 0-4)ceramics and investigated

J. Zhang · R. Zuo (✉) · Y. Lv
Institute of Electro Ceramics & Devices, School of Materials
Science and Engineering, Hefei University of Technology,
Hefei 230009, People's Republic of China
e-mail: piezolab@hfut.edu.cn

Y. Zhou · Z. Yue
State Key Lab of New Ceramics and Fine Processing,
Department of Materials Science and Engineering, Tsinghua
University, Beijing 100084, People's Republic of China

the effect of the substitution of $(Mg_{1/3}Nb_{2/3})^{4+}$ for Ti^{4+} on the microwave dielectric properties of BTN ceramic. To satisfy LTCC technology, $BaCu(B_2O_5)$ (BCB) has been widely used as a low-melting additive due to its low melting point ($\sim$850 °C) and good microwave dielectric properties ($\varepsilon_r \approx 7.4$, $Q \times f \approx 50{,}000$ GHz and $\tau_f \approx -32$ ppm/°C) [13–16]. However, no study has been so far reported about the effect of BCB on the sintering temperature and phase composition of BTN based ceramics [1, 17, 18]. In this work, we successfully developed a mid-permittivity LTCC microwave dielectrics based on BTMNN-x ceramics by using BCB as the sintering aid.

2 Experimental

Specimens of the BTMNN-x ceramics were prepared through a conventional solid-state reaction route using the high-purity oxide powders of $BaCO_3$, TiO_2, $(MgCO_3)_4$ $Mg(OH)_2 \cdot 5H_2O$, and Nb_2O_5. The stoichiometric mixture of the above raw materials were weighed and milled in ethanol medium for 24 h using zirconia balls. The slurry were dried and then calcined at 1,100 °C for 4 h. To synthesize the BCB ceramic powder, $Ba(OH)_2 \cdot 8H_2O$, CuO and H_3BO_3 were mixed for 24 h in a nylon jar with zirconia balls, and calcined at 800 °C for 12 h. The BTMNN-2 powders with 1.0–3.0 wt% BCB additives and 5 wt% PVA were re-milled for 24 h and were subsequently uniaxially pressed into cylinders of 10 mm in diameter and 6 mm in thickness. BTMNN-x samples were sintered in the temperature range of 1,190–1,320 °C for 4 h in air and the BCB doped BTMNN-2 samples were sintered at 875–1,000 °C for 2 h with a heating and cooling rate of 5 °C/min.

The bulk densities of the sintered specimens were measured by the Archimedes method. The crystal structures of sintered samples were determined by an X-ray powder diffractometer (XRD, Rigaku D/Max-II, Japan) using Cu Kα radiation. The microstructure of samples was observed by a scanning electron microscope (SEM, SSX-550, Shimadzu, Japan). An HP8720ES network analyzer (Hewlett-Packard, Santa Rosa, CA, USA) was used for the measurement of microwave dielectric properties by means of a Hakki–Coleman method [19, 20].

3 Results and discussion

Figure 1 shows the XRD patterns of BTMNN-x ceramics. It can be seen that all compositions exhibit single hexagonal structure as compared to the standard pattern of BTN (JCPDS card No. 70-1150), indicating that a complete solid solution was formed. Moreover, the diffraction peaks were
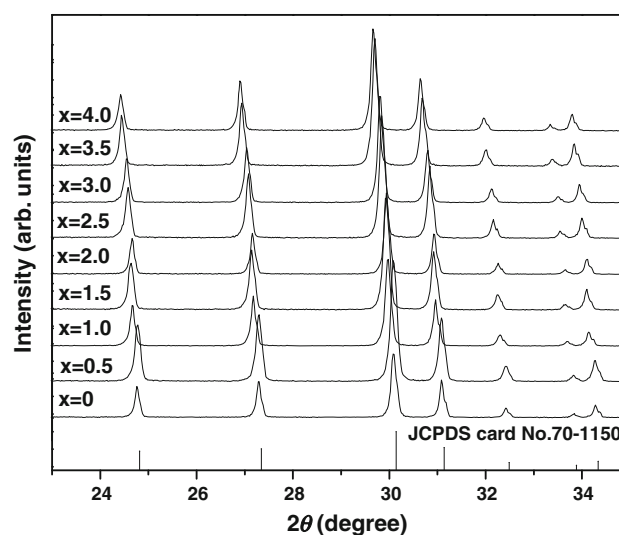

Fig. 1 XRD patterns of BTMNN-x ceramics ($0 \leq x \leq 4$) sintered at 1,270 °C for 4 h compared to a standard pattern of BTN

Table 1 The unit cell data and theoretical density of BTMNN-x ceramics calculated from the XRD results

x	a (Å)	c (Å)	Vol. per unit cell (Å^3)	Structure	Theoretical density (g/cm^3)
0	9.0503	11.7841	835.89	Hexagonal, Space group: P63/mcm (193)	5.211
0.5	9.0595	11.7958	838.43		5.239
1.0	9.0844	11.8243	845.09		5.241
1.5	9.0980	11.8460	849.17		5.259
2.0	9.1056	11.8599	851.59		5.288
2.5	9.1259	11.8853	857.22		5.296
3.0	9.1412	11.9014	861.26		5.314
3.5	9.1649	11.9319	867.95		5.315
4.0	9.1789	11.9509	871.99		5.333

found to shift toward the lower angles with increasing the substitution content x, owing to the expansion of unit cells. The lattice parameters calculated using XRD patterns are shown in Table 1. It can be seen that the unit-cell dimension of the hexagonal crystal structure increases after the substitution, which is mainly because the average ionic radius of $(Mg_{1/3}Nb_{2/3})^{4+}$ ($Mg^{2+} = 0.72$ Å, $Nb^{5+} = 0.64$ Å) is larger than that of Ti^{4+} (0.605 Å) [21]. According to the data of unit cell volume, the theoretical density values were calculated, which increase with x although the unit cell expands.

The relative densities of BTMNN-x ceramics sintered at different temperatures are shown in Fig. 2. It is obvious that the densification behavior of all samples was increased sharply with increasing the sintering temperature. After a maximum density value was reached, the density starts to decrease slightly with further increasing temperature,
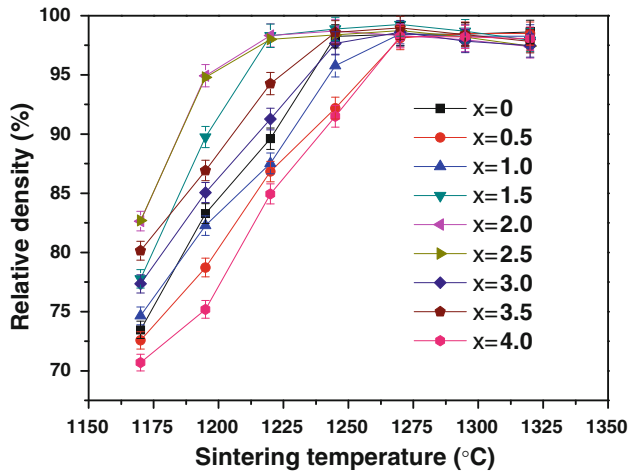
Fig. 2 Relative densities of BTMNN-x ceramics ($0 \le x \le 4$) sintered at different temperatures

Fig. 4 The dielectric constant (ε_r) and quality factor ($Q \times f$) of BTMNN-x ceramics ($0 \le x \le 4$) sintered at 1,270 °C for 4 h

probably owing to the rapid grain growth at excessively high sintering temperature. Moreover, it was found that Mg/Nb co-doping benefits to the reduction of the sintering temperature of BNT ceramics. The optimum sintering temperature can be reduced by ~ 100 °C for BTMNN-2 compared to undoped BTN. The SEM micrographs of BTMNN-x ceramics sintered at 1,270 °C are shown in Fig. 3. It was indicated that samples can be well densified at this temperature and have rod-like grains. The rapid grain growth behavior occurs in the sample as more Ti^{4+}

ions are replaced by Mg/Nb complex ions, meaning that the substitution tends to significantly promote the grain growth. This might be related to the fact that the expansion of the crystal lattice facilitates the mass transportation.

Figure 4 shows the dielectric constant (ε_r) and quality factor ($Q \times f$) values of BTMNN-x ceramics sintered at the optimum sintering temperatures. It can be seen that the ε_r value decreases from 66 for the BTMNN-0 sample to 41 for the BTMNN-4 sample, while the $Q \times f$ value increases from 10,500 to 22,500 GHz. As all measured samples had similar relative density values and no secondary phases were detected, the decrease in the permittivity value could

Fig. 3 SEM micrographs of BTMNN-x ceramics sintered at 1,270 °C for 4 h: **a** x = 0, **b** x = 1.5, **c** x = 2 and **d** x = 4
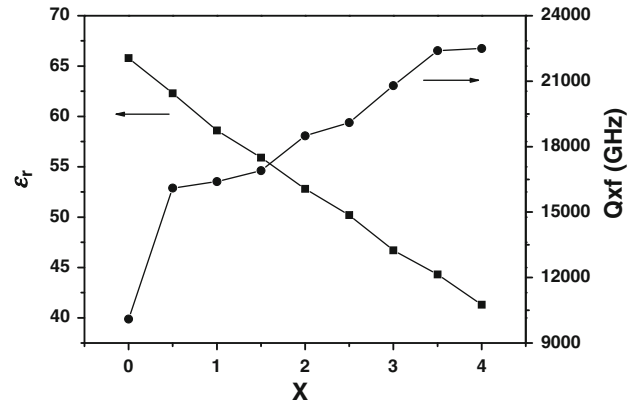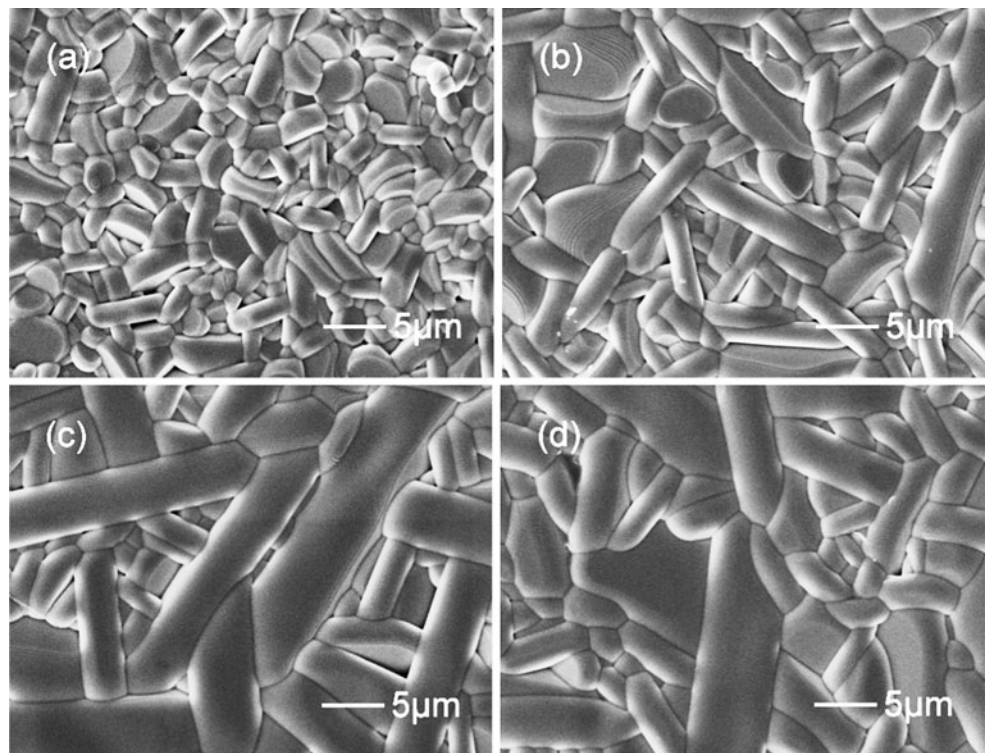
be attributed to the change of the crystal structure, particularly the molar volume (V_m) and ionic polarizability (α). The total molar dielectric polarizability of a compound can be simply calculated as a linear combination of individual ionic dielectric polarizabilities [22]. The molar dielectric polarizability would increase with the substitution of $(Mg_{1/3}Nb_{2/3})^{4+}$ for Ti^{4+} because of larger polarizability of $(Mg_{1/3}Nb_{2/3})^{4+}$ ($Mg^{2+} = 1.32$ Å^3, $Nb^{5+} = 3.97$ Å^3) than that of Ti^{4+} (2.93 Å^3) [22]. And the V_m value accordingly increases with increasing the substitution content (see Table 1) and changes faster than the α value does. This means the α/V_m values decrease with the increase of x. According to the Clausius–Mossotti equation [22]:

$$\frac{\varepsilon_r - 1}{\varepsilon_r + 2} = \left(\frac{4\pi}{3}\right)\left(\frac{\alpha}{V_m}\right) \tag{1}$$

the ε_r value would thus decline after the substitution as a result of the decrease in α/V_m values. The increase of the $Q \times f$ values seems to correlate with the increase of grain size. This can be supported by the observed relationship between the grain size versus dielectric loss [23]. Moreover, the dielectric loss in BTN ceramic was believed to be mainly ascribed to free electrons produced by defect equilibrium as described by the following reaction equations [24, 25]:

$$2O_o^x \Leftrightarrow 2V_o^{\bullet\bullet} + 4e' + O_2 \tag{2}$$

$$Ti_{Ti}^x + e' \Leftrightarrow Ti_{Ti}' \tag{3}$$

Therefore, the number of free electrons in BTMNN-x ceramics can be probably reduced with the substitution of $(Mg_{1/3}Nb_{2/3})^{4+}$ for Ti^{4+}. As a result, the $Q \times f$ values rise with the increase of the substitution.

Figure 5 illustrates the variation of the τ_f values of BTMNN-x ceramics with changing the substitution content x. It can be seen that the value of τ_f rapidly decreases from 56 ppm/°C for x = 0–15 ppm/°C for x = 4. It is known that τ_f is related to the thermal expansion coefficient α_l and the temperature coefficient of permittivity τ_ε [1], as follow:

$$\tau_f = -\left(\frac{1}{2}\tau_\varepsilon + \alpha_l\right) \tag{4}$$

However, because the thermal expansion coefficient usually has the negligible magnitude (~ 10 ppm/°C), τ_f actually depends on τ_ε. Bosman and Havinga [26] suggested that three effects could contribute to the τ_ε value, among which the direct dependence of the polarizability on temperature should play a major role because the other two effects are correlated to the volume expansion and have the same magnitude but are opposite in sign. In addition, a highly symmetric structure shows stronger temperature dependence of polarizability than a distorted structure [1]. The structure of BTMNN-x ceramics becomes more distorted with
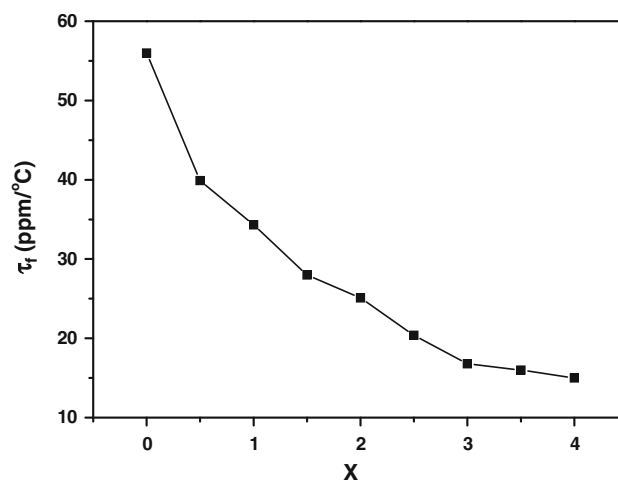

Fig. 5 The temperature coefficient τ_f of BTMNN-x ceramics sintered at 1,270 °C for 4 h

substituting $(Mg_{1/3}Nb_{2/3})^{4+}$ for Ti^{4+} because they have different ionic radius. As a result, the τ_ε value of the solid solution systems decreases with the increase of x.

Figure 6 shows the XRD patterns of BTMNN-2 ceramics doped with different amount of BCB additive (y = 1–3 wt%). It can be seen that samples doped with 1 and 1.5 wt% BCB still show single hexagonal structure. In addition, when y ≥ 2.0 wt%, a small amount of unknown secondary phases (marked with "?") start to appear and get strengthened with an increase of the BCB content. The results indicate that a small amount of BCB additive can enter into the lattice of BTMNN-2. However, it is interesting to note that the lattice parameters do not obviously change because detectable shift of diffraction peaks was not observed. Further increase of the BCB content would
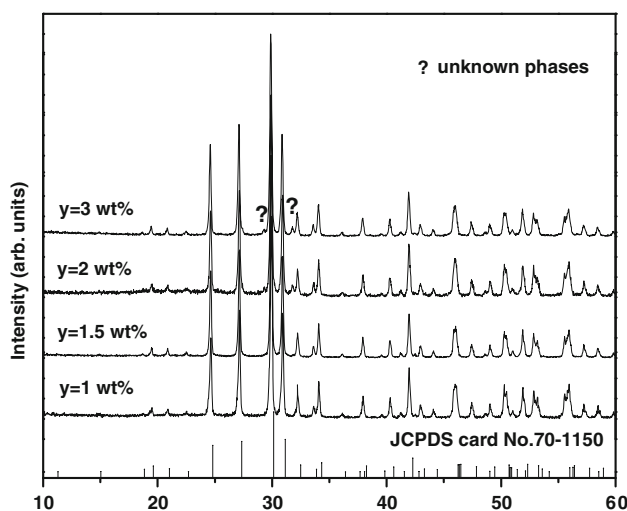

Fig. 6 XRD patterns of BTMNN-2 ceramics doped with y wt% BCB and sintered at 950 °C for 2 h
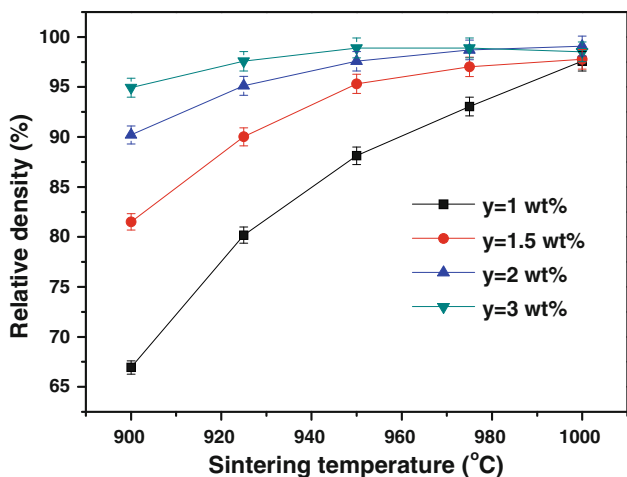
Fig. 7 Relative densities of BTMNN-2 ceramics doped with y wt% BCB and sintered at different temperatures

cause the presence of the secondary phases owing to the solubility limit.

The sintering behavior of BCB doped BTMNN-2 ceramics as a function of sintering temperature and the BCB content is shown in Fig. 7. It can be seen that the sample density strongly depends on the sintering temperature. Moreover, it increases obviously with the increase of the BCB content at a given sintering temperature. The 1.5 wt% BCB doped BTMNN-2 ceramics could reach more than 95% of the theoretical density, which reveals

that the addition of BCB can remarkably promote the densification behavior. Figure 8 shows the SEM micrographs of BTMNN-2 ceramics doped with various contents of BCB and sintered at 950 °C for 2 h. As can be seen, the microstructure gets more and more dense but grains grow only slightly. That is because BCB has a low melting point (~ 850 °C), it could become liquid at high temperature and promote the rearrangement of the particles and the mass transportation during sintering. The promotion of the densification behavior increases with doping more BCB additive although the secondary phases were detected as the BCB content was higher than 2 wt% (Fig. 6). However, impurity phases would have an adverse effect on the electrical properties.

The microwave dielectric properties of BCB doped BTMNN-2 ceramics are summarized in Table 2. Owing to the increase of the sample density, the ε_r value continuously increases with the BCB content and the sintering temperature. The Q × f values have the maximum values at y = 1.5 wt% and then decrease with further increase of the BCB content because of the presence of the secondary phases. In addition, the τ_f value decreases from 21 ppm/°C at y = 1 wt% to 16 ppm/°C at y = 3 wt%. This can be explained by the logarithmic mixture law for complex dielectrics that τ_f values can be tuned by mixing the dielectrics with opposite τ_f values [15]. BTMNN-2 ceramics possess a positive τ_f value of 25 ppm/°C (Fig. 5), and BCB ceramics were reported to exhibit a negative τ_f

Fig. 8 SEM micrographs of BCB doped BTMNN-2 ceramics sintered at 950 °C for 2 h: **a** y = 1 wt%, **b** y = 1.5 wt%, **c** y = 2 wt% and **d** y = 3 wt%
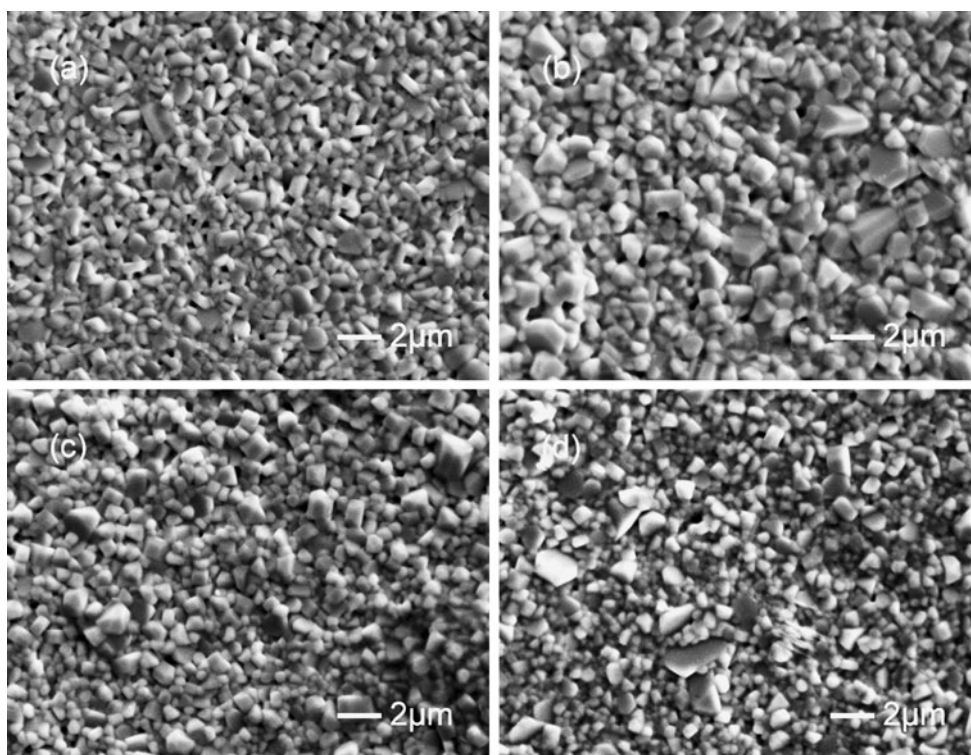
Table 2 The microwave dielectric properties of BCB doped BTMNN-2 ceramics sintered at 950 °C for 2 h

y (wt%)	ε_r	$Q \times f$ (GHz)	τ_f (ppm/°C)
1	45	9,500	21
1.5	50	10,500	18
2	53	5,600	17
3	55	2,800	16

value of −32 ppm/°C [13]. Thus, the τ_f value of BTMNN-2 ceramics decreases with increasing y. The BTMNN-2 ceramics doped with 1.5 wt% BCB and sintered at 950 °C for 2 h own good microwave dielectric properties of $\varepsilon_r = 50$, $Q \times f = 10,500$ GHz and $\tau_f = 18$ ppm/°C. These results indicate that BCB is an effective sintering aid for BTMNN system and simultaneously can keep desirable electrical properties.

4 Conclusion

Microwave dielectric ceramics of BTMNN solid solutions have been manufactured via a conventional solid-state reaction method. Complete solid solutions with single hexagonal structure have been identified. As a result of the substitution of $(Mg_{1/3}Nb_{2/3})^{4+}$ for Ti^{4+}, the ε_r and τ_f values decrease gradually, while the $Q \times f$ values increase from 10,500 GHz at x = 0–22,500 GHz at x = 4. In addition, BCB proves to be an effective sintering aid such that the 1 wt% BCB doped BTMNN-2 ceramics could be well densified at 950 °C and own desirable electrical properties of $\varepsilon_r = 50$, $Q \times f = 10,500$ GHz and $\tau_f = 18$ ppm/°C. These results indicated that the studied compositions could be applied for mid-permittivity LTCC materials.

References

1. Q.L. Zhang, D. Zou, H. Yang, J. Eur. Ceram. Soc. **31**, 265 (2011)
2. S.H. Wee, D.W. Kim, S.I. Yoo, J. Am. Ceram. Soc. **87**, 871 (2004)
3. Q.L. Zhang, H.J. Yang, Mater. Sci. Mater. Electron. **18**, 967 (2007)
4. M.Z. Jhou, J.H. Jean, J. Am. Ceram. Soc. **89**, 786 (2006)
5. J.X. Tong, Q.L. Zhang, H. Yang, J.L. Zou, Mater. Lett. **59**, 3252 (2005)
6. A.Y. Borisevich, P.K. Davies, J. Am. Ceram. Soc. **87**, 1047 (2004)
7. H. Zheng, I.M. Reaney, D. Muir, T. Price, D.M. Iddles, J. Eur. Ceram. Soc. **27**, 4479 (2007)
8. M.T. Sebastian, J. Mater. Sci. Mater. Electron. **10**, 475 (1999)
9. D. Groult, J.M. Chailleux, J. Choisnet, B. Raveau, J. Solid State Chem. **19**, 235 (1976)
10. W. Ko, Y. Choi, J. Korean Phys. Soc. **49**, 1234 (2006)
11. S. Rajesh, S.N. Babu, S.N. Potty, R. Ratheesh, Mater. Lett. **60**, 2179 (2006)
12. D. Zou, Q.L. Zhang, H. Yang, J. Mater. Sci. Mater. Electron. **20**, 756 (2009)
13. M.H. Kim, J.B. Lim, J.C. Kim, S. Nahm, J.H. Paik, J.H. Kim, K.S. Park, J. Am. Ceram. Soc. **89**, 3124 (2006)
14. X. Chen, H. Zhou, L. Fang, L. Liu, C. Li, R. Guo, H. Wang, Mater. Res. Bull. **45**, 1509 (2010)
15. L. Fang, D. Chu, C. Li, H. Zhou, Z. Yang, J. Am. Ceram. Soc. **94**, 524 (2011)
16. H. Jiang, J. Zhai, J. Zhang, X. Yao, J. Am. Ceram. Soc. **92**, 2319 (2009)
17. D.K. Yim, J.R. Kim, D.W. Kim, K.S. Hong, J. Eur. Ceram. Soc. **27**, 3053 (2007)
18. D. Zou, Q. Zhang, H. Yang, M. Ma, J. Mater. Sci. Mater. Electron. **19**, 1000 (2008)
19. B.W. Hakki, P.D. Coleman, IEEE Trans. Microwave Theory Tech. **8**, 402 (1960)
20. W.E. Courtney, IEEE Trans. Microwave Theory Tech. **18**, 476 (1970)
21. R.D. Shannon, Acta Cryst. A **32**, 751 (1976)
22. R.D. Shannon, J. Appl. Phys. **73**, 348 (1993)
23. S.J. Penn, N.M. Alford, A. Templeton, X. Wang, M. Xu, M. Reece, K. Schrapel, J. Am. Ceram. Soc. **80**, 1885 (1997)
24. W. Guoqing, W. Shunhua, S. Hao, Mater. Lett. **59**, 2229 (2005)
25. A. Templeton, X. Wang, S.J. Penn, S.J. Webb, L.F. Cohen, N.M. Alford, J. Am. Ceram. Soc. **83**, 95 (2000)
26. A.J. Bosman, E.E. Havinga, Phys. Rev. **129**, 1593 (1963)